PHILOSOPHICAL TRANSACTIONS OF THE ROYAL SOCIETY A MATHEMATICAL, PHYSICAL & ENGINEERING SCIENCES

Band structure and gaps of triangular graphene superlattices

F. Guinea and Tony Low

Phil. Trans. R. Soc. A 2010 **368**, 5391-5402
doi: 10.1098/rsta.2010.0214

PHILOSOPHICAL TRANSACTIONS OF THE ROYAL SOCIETY A

Phil. Trans. R. Soc. A (2010) **368**, 5391–5402
doi:10.1098/rsta.2010.0214

Review

Band structure and gaps of triangular graphene superlattices

By F. Guinea[1,*] and Tony Low[2]

[1]*Instituto de Ciencia de Materiales de Madrid, CSIC, Sor Juana Inés de la Cruz 3, 28049 Madrid, Spain*
[2]*Hall for Discovery Learning Research, Purdue University, West Lafayette, IN 47907-1791, USA*

The general properties of long wavelength triangular graphene superlattices are studied. It is shown that Dirac points with and without gaps can arise at a number of high-symmetry points of the Brillouin zone. The existence of gaps can lead to insulating behaviour at commensurate fillings. Strain and magnetic superlattices are also discussed.

Keywords: graphene; superlattices; electronic states

1. Introduction

Graphene is a two-dimensional metal when carriers are induced by an electric field (Novoselov *et al.* 2004, 2005; Geim & Novoselov 2007; Castro Neto *et al.* 2009). A gap at the Fermi level has been observed by scanning tunnelling microscopy measurements (Zhang *et al.* 2008; Li *et al.* 2009; see also Wehling *et al.* 2008). We analyse the gaps induced by a periodic structure, and the possibility that these gaps are generated spontaneously.

Graphene superlattices have been observed in graphene layers grown on transition metals (Vázquez de Parga *et al.* 2008; Borca *et al.* 2010; see also Oshima & Nagashima 1997; NDiaye *et al.* 2006; Marchini *et al.* 2007; Jiang *et al.* 2008; Martoccia *et al.* 2008; Pan *et al.* 2008; Usachov *et al.* 2008). Superlattices are also found in graphene grown by the decomposition of SiC (Zhou *et al.* 2007). In general, graphene superlattices can have interesting properties, such as highly anisotropic transport properties (Park *et al.* 2008*a*) or Dirac points at finite energies (Park *et al.* 2008*b*; Brey & Fertig 2009; Tiwari & Stroud 2009; Arovas *et al.* 2010; Barbier *et al.* 2010). In general, the study of the properties of graphene superlattices has attracted great interest, owing to the many novel features their electronic spectra can show (Pedersen *et al.* 2008; Abedpour *et al.* 2009; Bliokh *et al.* 2009; Gibertini *et al.* 2009; Park *et al.* 2009; Rosales *et al.* 2009; Shytov *et al.* 2009; Snyman 2009; Balog *et al.* 2010;

*Author for correspondence (paco.guinea@icmm.csic.es).

One contribution of 12 to a Theme Issue 'Electronic and photonic properties of graphene layers and carbon nanoribbons'.

da Silva-Araújo *et al.* 2010; Guinea *et al.* 2010). In the following, we analyse the general properties of the spectra of graphene superlattices with a two-dimensional triangular periodicity. These superlattices share the symmetries of the graphene lattice, and are commonly found in graphene layers grown on metallic surfaces. As discussed below, these superlattices can show a gap at the Fermi energy for a number of commensurate fillings. It seems probable that they can be formed spontaneously on very uniform substrates, such as BNi, or as a result of intrinsic instabilities of graphene.

In this paper, we study the general properties of triangular graphene superlattices created by a scalar potential, followed by a discussion of strain and magnetic superlattices.

2. Brillouin zone of triangular graphene superlattices

We define the lattice vectors of the graphene lattice as

$$\left.\begin{aligned} \boldsymbol{a}_1 &\equiv \mathbf{n}_x \\ \text{and} \quad \boldsymbol{a}_2 &\equiv \frac{1}{2}\mathbf{n}_x + \frac{\sqrt{3}}{2}\mathbf{n}_y. \end{aligned}\right\} \tag{2.1}$$

A triangular superlattice is described by the unit vectors

$$\left.\begin{aligned} \boldsymbol{b}_1 &\equiv n_1 \boldsymbol{a}_1 + n_2 \boldsymbol{a}_2 \\ \text{and} \quad \boldsymbol{b}_2 &\equiv -n_2 \boldsymbol{a}_1 + (n_1 + n_2)\boldsymbol{a}_2, \end{aligned}\right\} \tag{2.2}$$

where n_1 and n_2 are arbitrary integers different from zero.

There are three types of high-symmetry points in the Brillouin zone of a triangular lattice, Γ, M and K. There are two inequivalent K points, K and K′, at the corners of the hexagonal Brillouin zone, and three inequivalent M points, at the centres of the edges. Time reversal exchanges K and K′, while leaving the Γ point and the three M points unchanged (Mañes *et al.* 2007). The vectors that define these points are such that

$$\left.\begin{aligned} \boldsymbol{\Gamma}\,\boldsymbol{a}_1 = \boldsymbol{\Gamma}\,\boldsymbol{a}_2 &= 0, \\ \boldsymbol{K}\,\boldsymbol{a}_1 &= \frac{4\pi}{3}\,\boldsymbol{K}, \\ \boldsymbol{a}_2 &= \frac{2\pi}{3}, \\ \boldsymbol{K}'\,\boldsymbol{a}_1 &= \frac{2\pi}{3}\,\boldsymbol{K}', \\ \boldsymbol{a}_2 &= \frac{4\pi}{3}, \\ \boldsymbol{M}_1\,\boldsymbol{a}_1 = \pi\,\boldsymbol{M}_1\,\boldsymbol{a}_2 &= \pi, \\ \boldsymbol{M}_2\,\boldsymbol{a}_1 = \pi\,\boldsymbol{M}_2\,\boldsymbol{a}_2 &= 0 \\ \text{and} \quad \boldsymbol{M}_3\,\boldsymbol{a}_1 = 0\,\boldsymbol{M}_3\,\boldsymbol{a}_2 &= \pi. \end{aligned}\right\} \tag{2.3}$$

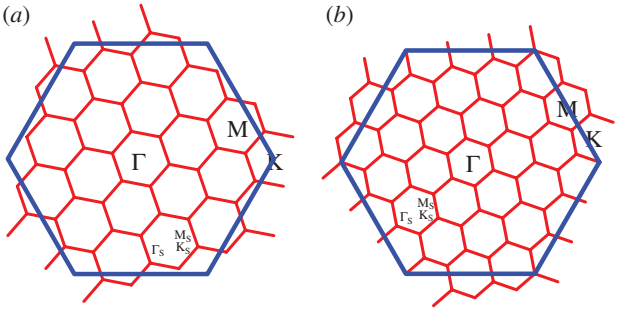

Figure 1. Examples of Brillouin zones of superlattices. (*a*) $n_1 = 1$ and $n_2 = 4$. (*b*) $n_1 = 2$ and $n_2 = 4$. (Online version in colour.)

The low-energy states of graphene lie close to the K and K′ of the original Brillouin zone. The positions of these points in the superlattice Brillouin zone are determined by

$$\left.\begin{aligned} \boldsymbol{K}_{\mathrm{S}}\boldsymbol{b}_1 &= \frac{4\pi}{3}n_1 + \frac{2\pi}{3}n_2, \quad \boldsymbol{K}_{\mathrm{S}}\boldsymbol{b}_2 = -\frac{4\pi}{3}n_2 + \frac{2\pi}{3}(n_1+n_2) \\ \text{and} \qquad \boldsymbol{K}'_{\mathrm{S}}\boldsymbol{b}_1 &= \frac{2\pi}{3}n_1 + \frac{4\pi}{3}n_2, \quad \boldsymbol{K}'_{\mathrm{S}}\boldsymbol{b}_2 = -\frac{2\pi}{3}n_2 + \frac{4\pi}{3}(n_1+n_2). \end{aligned}\right\} \tag{2.4}$$

Thus, when $2n_1 + n_2$ is a multiple of three, the graphene K and K′ points will be mapped onto the Γ_{S} point of the superlattice Brillouin zone. Otherwise, they will be mapped onto the corners of the Brillouin zone, K_{S} and K'_{S}. Examples of superlattice Brillouin zones are given in figure 1.

3. Dispersion near high-symmetry points

(*a*) *The model*

We study superlattices induced by a modulation of the on-site energy of the π orbitals. We assume that it is a weak perturbation of the graphene Dirac equation, except in cases where degeneracies occur. We consider the Fourier components of the potential with lowest wavevector, of modulus

$$G = \frac{4\pi}{a\sqrt{3(n_1^2 + n_2^2 + n_1 n_2)}}. \tag{3.1}$$

We write the potential as the sum of symmetric part V_G, and an antisymmetric part, Δ_G, with respect to the interchange of sublattices. We neglect for the moment the short wavelength components that mix the two inequivalent Dirac points of the unperturbed graphene layer.

We analyse the changes in the Fermi velocity near the Dirac energy induced by the superlattice potential, and the points in the lowest bands of the superlattice where degeneracies persist when $V_G \neq 0$ and $\Delta_G = 0$. As discussed below, this situation gives rise to a new set of Dirac equations at finite energies.

(*b*) *Dirac energy at the* $\Gamma_{\rm S}$ *point*

We consider the case when the K and K′ points of the graphene Brillouin zone are mapped onto the $\Gamma_{\rm S}$ point of the superlattice Brillouin zone. Using lowest order perturbation theory, we find, near the $\Gamma_{\rm S}$ point, a renormalization of the Fermi velocity (Park *et al.* 2008*a*,*b*)

$$\delta v_{\rm F}(\boldsymbol{k}) \approx \sum_{\boldsymbol{G}} -\frac{V_{\boldsymbol{G}}^2 + \Delta_{\boldsymbol{G}}^2}{v_{\rm F}|\boldsymbol{G}|^2} + \frac{V_{\boldsymbol{G}}^2 - \Delta_{\boldsymbol{G}}^2}{v_{\rm F}|\boldsymbol{G}|^2}[\cos^2(\phi_{\boldsymbol{k},\boldsymbol{G}}) - \sin^2(\phi_{\boldsymbol{k},\boldsymbol{G}})], \tag{3.2}$$

where $\phi_{\boldsymbol{k},\boldsymbol{G}}$ is the angle between vectors $\boldsymbol{k}$ and $\boldsymbol{G}$. For the hexagonal superlattice considered here we find the isotropic reduction in the Fermi velocity

$$\delta v_{\rm F} \approx -\frac{6|V_G|^2}{v_{\rm F} G^2} - \frac{6|\Delta_G|^2}{v_{\rm F} G^2}. \tag{3.3}$$

There is a twofold degeneracy at the three $\rm M_S$ points, if $\Delta_G = 0$. The energy of these states is $v_{\rm F} G/2$. At finite distances from the $\rm M_S$ points, we can write an effective hamiltonian,

$$H \equiv \begin{pmatrix} \dfrac{v_{\rm F} G}{2} + 2 v_{\rm F} k_x & \Delta_G + \dfrac{4{\rm i} V_G k_y}{G} \\ \Delta_G - \dfrac{4{\rm i} V_G k_y}{G} & \dfrac{v_{\rm F} G}{2} - v_{\rm F} k_x \end{pmatrix}, \tag{3.4}$$

which gives an anisotropic Dirac equation with a gap,

$$\epsilon_{\rm M_S} \approx \frac{v_{\rm F} G}{2} \pm \sqrt{4 v_{\rm F}^2 k_x^2 + \Delta_G^2 + \frac{16 V_G^2 k_y^2}{G^2}}. \tag{3.5}$$

At the $\rm K_S$ and $\rm K_S'$ points, there are three degenerate levels for $V_G = \Delta_G = 0$, with energy $\epsilon_{\rm K_S} = v_{\rm F} G/\sqrt{3}$. When $V_G \neq 0$, these three levels are split into a doublet, with energy $\epsilon^d_{\rm K_S} = v_{\rm F} G/\sqrt{3} + V_G/2$, and a singlet, at $\epsilon^s_{\rm K_S} = v_{\rm F} G/\sqrt{3} - V_G$. Expanding around the $\rm K_S$ point, the effective hamiltonian for the doublet is

$$H \equiv \begin{pmatrix} \dfrac{v_{\rm F} G}{\sqrt{3}} + \dfrac{V_G}{2} - \dfrac{v_{\rm F} k_x}{2} & \dfrac{v_{\rm F} k_y}{2} - \dfrac{3{\rm i}\Delta_G}{4} \\ \dfrac{v_{\rm F} k_y}{2} + \dfrac{3{\rm i}\Delta_G}{4} & \dfrac{v_{\rm F} G}{\sqrt{3}} + \dfrac{V_G}{2} + \dfrac{v_{\rm F} k_x}{2} \end{pmatrix}. \tag{3.6}$$

This is the two-dimensional Dirac equation with a mass term. The dispersion relation is

$$\left.\begin{aligned} \epsilon^s_{\rm K_S} &\approx \frac{v_{\rm F} G}{\sqrt{3}} - V_G + O\left(\frac{\Delta_G^2}{V_G}, \frac{v_{\rm F}^2 (k_x^2 + k_y^2)}{V_G}\right) \\ \text{and} \quad \epsilon^d_{\rm K_S} &\approx \frac{v_{\rm F} G}{\sqrt{3}} + \frac{V_G}{2} \pm \sqrt{\frac{v_{\rm F}^2 (k_x^2 + k_y^2)}{4} + \frac{9\Delta_G^2}{16}}. \end{aligned}\right\} \tag{3.7}$$

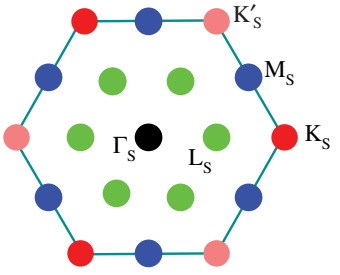

Figure 2. Points in the superlattice Brillouin zone where degeneracies occur when $V_G \neq 0$. (Online version in colour.)

There are two sets of degenerate bands, derived from the K and K′ points of the Brillouin zone of graphene. This degeneracy will be broken by short wavelength terms in the superlattice potential.

(*c*) *Dirac energy at the* $\mathrm{K_S}$ *and* $\mathrm{K'_S}$ *points*

The renormalization of the Fermi velocity near the $\mathrm{K_S}$ and $\mathrm{K'_S}$ points is the same as in equation (3.3).

There are doubly degenerate states, even when $V_G \neq 0$, at the six inequivalent points at positions $\boldsymbol{L}_\mathrm{S} = \boldsymbol{K}_\mathrm{S}/2$, as shown in figure 2. The energy of these points is $\epsilon_{\mathrm{L_S}} = v_\mathrm{F} G/2$. Expanding around these points, we find an effective anisotropic Dirac equation, given by equation (3.4).

There is another set of doubly degenerate states at the $\mathrm{M_S}$ points. The two states arise from the K and K′ points of the original graphene Brillouin zone. The degeneracy persists when $V_G \neq 0$ and $\Delta_G \neq 0$, and is broken only by short wavelength components of the superlattice potential. When these components are finite, an effective anisotropic Dirac equation will arise similar to that in equation (3.4).

For $V_G = \Delta_G = 0$, there are six degenerate states at the Γ_S point. The long-range part of the superlattice potential will hybridize states that are derived from the K and K′ points of the original graphene Brillouin zone. We obtain two sets of isotropic Dirac equations, described by equation (3.6), and two degenerate states. The short-range part of the Dirac equation will break these degeneracies.

(*d*) *Results*

We analyse the bands induced by an $N \times N$ superlattice. The hopping matrix between π orbitals in neighbouring carbon atoms is $t = 3\,\mathrm{eV}$. The bands for $V_G = 0.3\,\mathrm{eV}$ and $\Delta_G = 0$ are shown in figure 3. The bands show Dirac points at the $\mathrm{M_S}$ and $\mathrm{K_S}$ points. When Δ_G is increased to $\Delta_G = 0.1\,\mathrm{eV}$, a gap appears between successive bands, as shown in figure 4. The density of states for those two cases is shown in figure 5. Note that the potential breaks the electron–hole symmetry of clean graphene, and the gaps are not of the same magnitude for positive and negative energies.

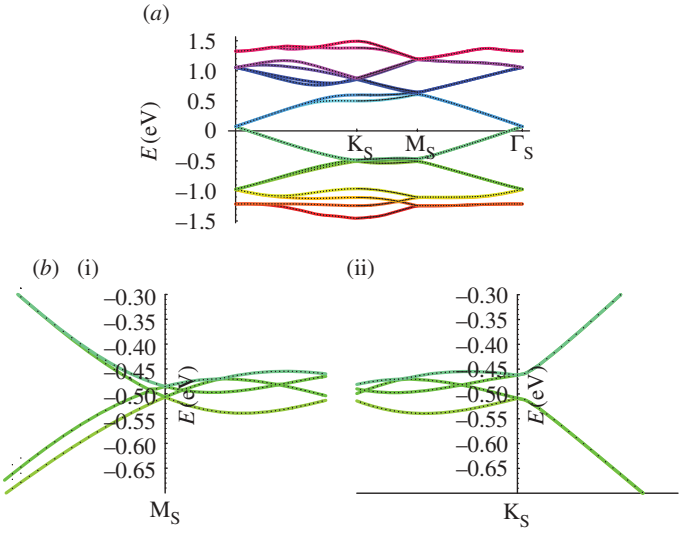

Figure 3. (*a*) Low-energy bands for a 12×12 superlattice, with $V_G = 0.3\,\mathrm{eV}$ and $\Delta_G = 0$. (*b*)(i) Detail near the $\mathrm{M_S}$ point. (ii) Detail near the $\mathrm{K_S}$ point. (Online version in colour.)

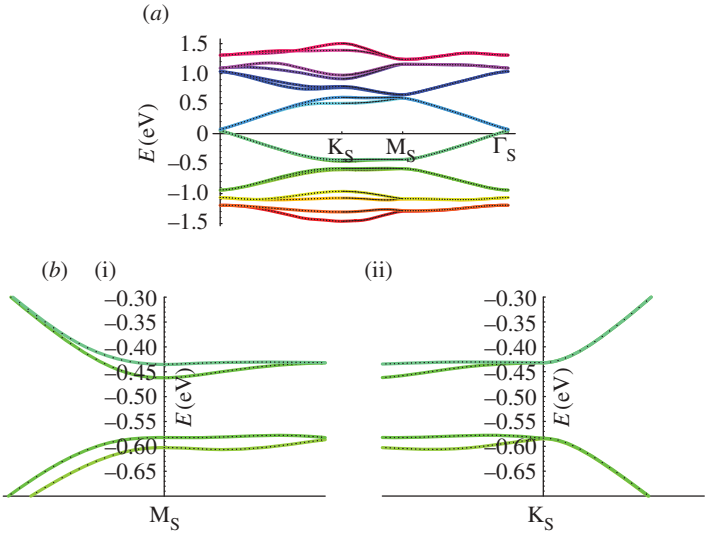

Figure 4. (*a*) Low-energy bands for a 12×12 superlattice, with $V_G = 0.3\,\mathrm{eV}$ and $\Delta_G = 0.1\,\mathrm{eV}$. (*b*)(i) Detail near the $\mathrm{M_S}$ point. (ii) Detail near the $\mathrm{K_S}$ point. (Online version in colour.)

The results are in reasonable agreement with the analytical description in the previous section. A gap of order $2\Delta_G$ is induced at the $\mathrm{M_S}$ point. In order for this gap to be possible, the following inequalities must be satisfied:

$$\left.\begin{aligned} &\epsilon^{s}_{\mathrm{K_S}} \approx \frac{v_{\mathrm{F}} G}{\sqrt{3}} - V_G \leq \epsilon^{-}_{\mathrm{M_S}} \approx \frac{v_{\mathrm{F}} G}{2} - \Delta_G \\ \text{and} \quad &\epsilon^{+}_{\mathrm{M_S}} \approx \frac{v_{\mathrm{F}} G}{2} + \Delta_G \leq \epsilon^{d}_{\mathrm{K_S}} \approx \frac{v_{\mathrm{F}} G}{\sqrt{3}} + \frac{V_G}{2} - \frac{3\Delta_G}{4}. \end{aligned}\right\} \tag{3.8}$$

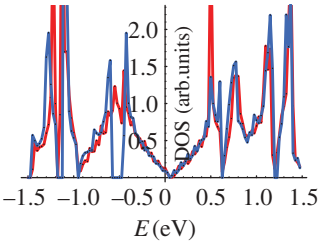

Figure 5. Density of states (DOS) for a 12×12 superlattice. Black, $V_G = 0.3\,\mathrm{eV}$ and $\Delta_G = 0$; grey, $V_G = 0.3\,\mathrm{eV}$ and $\Delta_G = 0.1\,\mathrm{eV}$. (Online version in colour.)

The scaling properties of the Dirac equation imply that, if the dimension of the superlattice is increased, $G \to \lambda G$, with $\lambda < 1$, then a rescaling of the superlattice potential, $V_G \to \lambda V_G, \Delta_G \to \lambda \Delta_G$, will lead to the same band structure, with energies scaled as $E \to \lambda E$.

4. Strain superlattices

A superlattice can also be produced by inducing strains, which modulate the interatomic hoppings. The corresponding perturbation can be seen as a gauge field, $\boldsymbol{A}$, which shifts locally the momentum (Vozmediano *et al.* 2010). A simple case is when the strains are due to height modulations, $h(\boldsymbol{r})$, which can be induced by a substrate. In terms of the Fourier components of the modulation, $h_{\boldsymbol{G}}$, and allowing for the relaxation of the in-plane displacements, the effective gauge field can be written as (Guinea *et al.* 2008)

$$\left.\begin{aligned} A_x(\boldsymbol{G}) &= \frac{\beta}{a}\frac{(\lambda+\mu)(G_x^2-G_y^2)[h^{xx}_{\boldsymbol{G}}G_y^2-(h^{xy}_{\boldsymbol{G}}+h^{yx}_{\boldsymbol{G}})G_xG_y+h^{yy}_{\boldsymbol{G}}G_x^2]}{|\boldsymbol{G}|^4(\lambda+2\mu)} \\ \text{and}\quad A_y(\boldsymbol{G}) &= \frac{\beta}{a}\frac{(\lambda+\mu)2G_xG_y[h^{xx}_{\boldsymbol{G}}G_y^2-(h^{xy}_{\boldsymbol{G}}+h^{yx}_{\boldsymbol{G}})G_xG_y+h^{yy}_{\boldsymbol{G}}G_x^2]}{|\boldsymbol{G}|^4(\lambda+2\mu)}, \end{aligned}\right\} \tag{4.1}$$

where $\beta = \partial \log(t)/\partial \log(a) \approx 2-3$, $t \approx 3\,\mathrm{eV}$ is the hopping between nearest neighbour π orbitals, $a \approx 1.4\,\text{Å}$ is the distance between nearest neighbour carbon atoms, and the tensor $h^{ij}_{\boldsymbol{G}}$ is the Fourier transform of the functions

$$h^{ij}(\boldsymbol{r}) = \frac{\partial h}{\partial x_i}\frac{\partial h}{\partial x_j} \tag{4.2}$$

and λ and μ are the elastic Lamé coefficients of graphene. The field in equation (4.1) has opposite signs in the two valleys in the Brillouin zone.

The calculation of the effective magnetic field induced by the gauge field in equation (4.1) is simplified when, as in the previous sections, only one component, $h(\boldsymbol{r}) = h_G \sum_{l=1,\ldots,6} \mathrm{e}^{\mathrm{i}\boldsymbol{G}_l\boldsymbol{r}}$, in a superlattice is considered. The tensor in equation (4.2) has non-zero components for all combinations of the type $\boldsymbol{G}_k + \boldsymbol{G}_l$. When the gauge field $\boldsymbol{A}(\boldsymbol{G})$ is parallel to $\boldsymbol{G}$, the vector potential can be gauged away, and does not induce an effective magnetic field. This implies that out of

the 18 possible values of the vector $\boldsymbol{G}_k + \boldsymbol{G}_l$, only six possible values contribute to the effective magnetic field. These vectors are given by $\boldsymbol{G} \equiv G(3/2, \sqrt{3}/2)$ and the vectors equivalent to it by a symmetry transformation. After some algebra, we obtain for the effective magnetic field

$$B_{\rm strain}(\boldsymbol{r}) = \frac{\beta}{a}\frac{\lambda+\mu}{\lambda+2\mu}\frac{27\sqrt{3}}{8}G^3 h_G^2\left[2\cos(\sqrt{3}Gy) + 4\cos\left(\frac{\sqrt{3}Gy}{2}\right)\cos\left(\frac{3Gx}{2}\right)\right]. \tag{4.3}$$

The superlattice defined by the effective magnetic field has a unit vector of length $\sqrt{3}G$, so that the area of its unit cell is smaller than the area of the unit cell of the original superlattice by a factor 1/3.

Using equation (4.3) and $G = 2\pi/L$, where L is the length of the unit vector of the superlattice, we can write the magnetic length associated with the maximum effective field in the system as

$$\frac{1}{\ell_{\rm B}^2} = \frac{\lambda+\mu}{\lambda+2\mu}\frac{\beta}{a}\frac{9\sqrt{3}\pi^3}{2}\frac{h_{\rm max}^2}{L^3}, \tag{4.4}$$

where $h_{\rm max} = 6h_G$ is the maximum value of $h(\boldsymbol{G})$, assuming $h_G > 0$. For values $h_{\rm max} \approx 1\,{\rm nm}$ and $L \approx 40\,{\rm nm}$, we find $l_{\rm B} \approx 14\,{\rm nm}$, so that the effective field is such that $B_{\rm strain}^{\rm max} \approx 1$–$2\,{\rm T}$.

5. Magnetic superlattices

A superlattice can also be induced by a spatially modulated magnetic field. A combination of a modulated magnetic field and a scalar potential opens a gap at the Dirac energy, and the resulting insulator is a quantum Hall system (Snyman 2009), with chiral currents at the boundaries (Haldane 1988). Here, we obtain this effect using second-order perturbation theory, instead of the arguments used in Snyman (2009). As in the previous sections, we assume the simplest periodicity compatible with the superlattice hexagonal symmetry

$$\left.\begin{aligned} V(\boldsymbol{r}) &= V_G \sum_{l=1,\cdots,6} {\rm e}^{{\rm i}\boldsymbol{G}_l\boldsymbol{r}} \\ \text{and} \qquad B(\boldsymbol{r}) &= B_G \sum_{l=1,\cdots,6} {\rm e}^{{\rm i}\boldsymbol{G}_l\boldsymbol{r}}. \end{aligned}\right\} \tag{5.1}$$

The eigenstates of the unperturbed Hamiltonian at the K and K′ points of the Brillouin zone can be written as $|0\rangle_A = (1,0)$ and $|0\rangle_{\rm B} = (0,1)$, of which each component of the spinor corresponds to one sublattice. These states are hybridized with states $|\boldsymbol{G}_\pm\rangle_{\rm K} = (1, \pm{\rm e}^{{\rm i}\phi_{\boldsymbol{G}}})$ and $|\boldsymbol{G}_\pm\rangle_{\rm K'} = (1, \mp{\rm e}^{-{\rm i}\phi_{\boldsymbol{G}}})$, with energies $\epsilon_{\boldsymbol{G}} = \pm v_{\rm F}|\boldsymbol{G}|$ and ${\rm e}^{{\rm i}\phi_{\boldsymbol{G}}} = (G_x + {\rm i}G_y)/|\boldsymbol{G}|$.

The energies of states $|0\rangle_A$ and $|0\rangle_{\rm B}$ are modified in different ways by virtual hoppings into states $|\boldsymbol{G}_\pm\rangle_{\rm K}$ and $|\boldsymbol{G}_\pm\rangle_{\rm K'}$, leading to gaps in both valleys. Moreover, the gaps have different signs, showing that the time reversal symmetry in the system is broken, and that a quantum Hall phase has been induced. The gap can

be written as

$$\Delta = \pm \sum_{l=1,\ldots,6} \frac{2v_{\mathrm{F}}\mathrm{Re}\{V^{*}_{\boldsymbol{G}_l}[A_x(\boldsymbol{G}_l) + \mathrm{i}A_y(\boldsymbol{G}_l)]\mathrm{e}^{-\mathrm{i}\phi_{\boldsymbol{G}_l}}\}}{|\epsilon_{\boldsymbol{G}_l}|}, \tag{5.2}$$

where $\boldsymbol{A}_{\boldsymbol{G}}$ is the vector potential, which we define as

$$\left.\begin{aligned} A_x(\boldsymbol{G}) &= \frac{\mathrm{i}G_y}{|\boldsymbol{G}|^2}\frac{B_{\boldsymbol{G}}}{\Phi_0} \\ \text{and} \qquad A_y(\boldsymbol{G}) &= \frac{-\mathrm{i}G_x}{|\boldsymbol{G}|^2}\frac{B_{\boldsymbol{G}}}{\Phi_0}, \end{aligned}\right\} \tag{5.3}$$

where $\Phi_0 = eh/c$ is the quantum unit of flux. Using this expression, we finally obtain

$$\Delta = 12\frac{B_G V_G}{\Phi_0 G^2} \tag{5.4}$$

in agreement with Snyman (2009).

6. Self-consistent opening of a gap

The previous analysis shows that a gap can open at finite energies in graphene in the presence of a superlattice potential with a staggered component. When the number of carriers is such that only a small number of subbands are completely filled and the rest are completely empty the electronic energy will be lowered in the presence of the gap. A lattice distortion that leads to the appropriate potential will be energetically favourable if the gain in electronic energy exceeds the formation energy of the distortion, as in the Peierls instability in one dimension.

In graphene on top of a metal or other substrate with a large dielectric constant, as in Vázquez de Parga *et al.* (2008), out-of-plane displacements lead to changes in the on-site energies of the π orbitals. An electron in a given carbon atom experiences the image potential owing to the screening. A change in position of Δz leads to a change in the image potential of order $ee^{*}\Delta z/(4d^2)$, where $e^{*} = e(\epsilon_0 - 1)/(\epsilon_0 + 1)$ is the image charge, ϵ_0 is the dielectric constant of the substrate and d is the distance to the substrate. A vertical displacement of $\Delta z \sim 1$ Å when the graphene layer is at a distance $d \approx 3$ Å of the substrate can lead to shifts of the on-site energies of order 0.1 eV. The electronic gain of energy owing to the existence of a gap, per unit cell, is then $E_{\mathrm{elec}} \approx \Delta_G \approx ee^{*}\Delta z d^{-2}$.

The elastic energy per unit cell required to create a staggered distortion of amplitude Δz is of order $E_{\mathrm{elas}} \approx \kappa \Delta z^2 a^{-2}$, where $\kappa \approx 1$ eV is the bending rigidity of graphene.

A gap will exist above a threshold for the superlattice potential, $V_G \sim \Delta_G \gtrsim v_{\mathrm{F}} G(1/\sqrt{3} - 1/2)$. The area of the Brillouin zone of the supercell, $\sqrt{3}G^2/2$, should be close to the area within the Fermi surface of the unperturbed graphene, πk_{F}^2.

Hence, a spontaneous staggered distortion is favoured if

$$\left.\begin{aligned} E_{\rm elec} + E_{\rm elas} &\approx -\frac{ee^*\Delta z}{d^2} + \kappa\left(\frac{\Delta z}{a}\right)^2 < 0, \\ V_G &\approx \frac{ee^*\Delta z}{d^2} > v_{\rm F} G\left(\frac{1}{\sqrt{3}} - \frac{1}{2}\right) \\ \text{and} \qquad \frac{\sqrt{3}G^2}{2} &\approx \pi k_{\rm F}^2. \end{aligned}\right\} \tag{6.1}$$

The last equation in (6.1) implies that $G \propto k_{\rm F}$, and from the first two we obtain that $v_{\rm F} G \lesssim (ee^*)^2 a^2 d^{-4} \kappa^{-1}$. Hence, a spontaneous distortion is energetically favoured for carrier densities such that

$$\rho = \pi k_{\rm F}^2 \lesssim \frac{(ee^*)^4 a^4}{v_{\rm F}^2 \kappa^2 d^8} \tag{6.2}$$

and the staggered distortion, with inverse wavelength $G \sim k_{\rm F}$ of the order

$$\Delta z \sim \frac{v_{\rm F} k_{\rm F} d^2}{ee^*}. \tag{6.3}$$

For a metal, we have $e_0 = \infty$ and $e^* = e$. For $a \approx 2\,$Å, $d \approx 3\,$Å and $\kappa \approx 1\,$eV, we find that a staggered corrugation is energetically favoured for carrier densities $\rho \lesssim 10^{13}\,{\rm cm}^{-2}$, leading to maximum deformations of 0.2 Å. For SiO_2, where $\epsilon_0 = 3.9$ and $e^* \approx 0.6e$, the corrugations take place for carrier densities $\rho \lesssim 3 \times 10^{12}\,{\rm cm}^{-2}$, and maximum deformations of 0.15 Å.

The formation of these long wavelength modulations is only possible in systems with a high degree of order, as the superlattice features will be reduced by disorder. For instance, weak scatterers with concentration $n_{\rm imp}$, which change the on-site potential by an amount of order Δ_G, lead to a mean free path $l_{\rm el} \sim v_{\rm F}^2/(\Delta_G^2 k_{\rm F} a^4 n_{\rm imp})$. A large concentration of these defects, $n_{\rm imp} \sim a^{-2}$, will suppress the formation of a superlattice, while little affecting the conductivity, $\sigma \sim (e^2/h) \times (k_{\rm F} l_{\rm el}) \sim (e^2/h) \times (v_{\rm F}^2 a^{-2} \Delta_G^{-2})$.

7. Conclusion

We have analysed the formation of Dirac points and gaps at high-energy points of triangular graphene superlattices. We have shown that, in some cases, a gap can be formed over the entire Fermi surface, making graphene insulating. We have discussed instabilities that might give rise to the spontaneous formation of gaps of this type. General properties of strain and magnetic superlattices have also been discussed.

We appreciate useful conversations with J. L. Mañes, R. Miranda and A. Vázquez de Praga. Funding from MICINN (Spain) through grants FIS2008-00124 and CONSOLIDER CSD2007-00010 is gratefully acknowledged. T.L. acknowledges funding from INDEX/NSF (US).

References

Abedpour, N., Esmailpour, A., Asgari, R. & Tabar, M. R. 2009 Conductance of disordered graphene superlattice. *Phys. Rev. B* **79**, 165412. (doi:10.1103/PhysRevB.79.165412)

Arovas, D. P., Brey, L., Fertig, H. A., Kim, E.-A. & Ziegler, K. 2010 Dirac spectrum in piecewise constant one-dimensional potentials. (http://arxiv.org/abs/1002.3655).

Balog, R. *et al.* 2010 Bandgap opening in graphene induced by patterned hydrogen adsorption. *Nat. Mat.* **9**, 315. (doi:10.1038/nmat2710)

Barbier, M., Vasilopoulos, P. & Peeters, F. M. 2010 Extra dirac points in the energy spectrum for superlattices on single-layer graphene. (http://arxiv.org/abs/1002.1442v1).

Bliokh, Y. P., Freilikher, V., Savel'ev, S. & Nori, F. 2009 Transport and localization in periodic and disordered graphene superlattices. *Phys. Rev. B* **79**, 075123. (doi:10.1103/PhysRevB.79.075123)

Borca, B., *et al.* 2010 Electronic and geometric corrugation of periodically rippled, self-nanostructured graphene epitaxially grown on Ru(0001). (http://arxiv.org/abs/1005.1764).

Brey, L. & Fertig, H. A. 2009 Emerging zero modes for graphene in a periodic potential. *Phys. Rev. Lett.* **103**, 046809. (doi:10.1103/PhysRevLett.103.046809)

Castro Neto, A. H., Guinea, F., Peres, N. M. R., Novoselov, K. S. & Geim, A. K. 2009 The electronic properties of graphene. *Rev. Mod. Phys.* **81**, 109. (doi:10.1103/RevModPhys.81.109)

da Silva-Araújo, J., Chacham, H. & Nunes, R. W. 2010 Gap opening in topological-defect lattices in graphene. *Phys. Rev. B* **81**, 193405. (doi:10.1103/PhysRevB.81.193405)

Geim, A. K. & Novoselov, K. S. 2007 The rise of graphene. *Nat. Mater.* **6**, 183. (doi:10.1038/nmat1849)

Gibertini, M., Singha, A., Pellegrini, V., Polini, M., Vignale, G., Pinczuk, A., Pfeiffer, L. N. & West, K. W. 2009 Engineering artificial graphene in a two-dimensional electron gas. *Phys. Rev. B* **79**, 241406. (doi:10.1103/PhysRevB.79.241406)

Guinea, F., Horovitz, B. & Doussal, P. L. 2008 Gauge field induced by ripples in graphene. *Phys. Rev. B* **77**, 205421. (doi:10.1103/PhysRevB.77.205421)

Guinea, F., Katsnelson, M. I. & Geim, A. K. 2010 Energy gaps, topological insulator state and zero-field quantum Hall effect in graphene by strain engineering. *Nat. Phys.* **6**, 30. (doi:10.1038/nphys1420)

Haldane, F. D. M. 1988 Model for a quantum Hall effect without landau levels: condensed-matter realization of the 'parity anomaly'. *Phys. Rev. Lett.* **61**, 2015. (doi:10.1103/PhysRevLett.61.2015)

Jiang, D.-E., Du, M.-H. & Dai, S. 2008 First principles study of the graphene/Ru(0001) interface. (http://arxiv.org/abs/0901.1101).

Li, G., Luican, A. & Andrei, E. Y. 2009 Scanning tunneling spectroscopy of graphene. *Phys. Rev. Lett.* **102**, 176804. (doi:10.1103/PhysRevLett.102.176804)

Mañes, J. L., Guinea, F. & Vozmediano, M. A. H. 2007 Existence and topological stability of Fermi points in multilayered graphene. *Phys. Rev. B* **75**, 155424. (doi:10.1103/PhysRevB.75.155424)

Marchini, S., Günther, S. & Wintterlin, J. 2007 Scanning tunneling microscopy of graphene on Ru(0001). *Phys. Rev. B* **76**, 075429. (doi:10.1103/PhysRevB.76.075429)

Martoccia, D., *et al.* 2008 Graphene on Ru(0001): a 25×25 supercell. *Phys. Rev. Lett.* **101**, 126102. (doi:10.1103/PhysRevLett.101.126102)

NDiaye, A. T., Bleikamp, S., Feibelman, P. J. & Michely, T. 2006 Two-dimensional ir cluster lattice on a graphene Moiré on Ir(111). *Phys. Rev. Lett.* **97**, 215501. (doi:10.1103/PhysRevLett.97.215501)

Novoselov, K. S., Geim, A. K., Morozov, S. V., Jiang, D., Zhang, Y., Dubonos, S. V., Grigorieva, I. V., & Firsov, A. A. 2004 Electric field effect in atomically thin carbon films. *Science* **306**, 666. (doi:10.1126/science.1102896)

Novoselov, K. S., Jiang, D., Schedin, F., Booth, T. J., Khotkevich, V. V., Morozov, S. V. & Geim, A. K. 2005 Two-dimensional atomic crystals. *Proc. Natl Acad. Sci. USA* **102**, 10451. (doi:10.1073/pnas.0502848102)

Oshima, C. & Nagashima, A. 1997 Ultra-thin epitaxial films of graphite and hexagonal boron nitride on solid surfaces. *J. Phys. Condens. Matter* **9**, 1. (doi:10.1088/0953-8984/9/1/004)

Pan, Y., Jiang, N., Sun, J. T., Shi, D. X., Du, S. X., Liu, F. & Gao, H.-J. 2008 Millimeter-scale, highly ordered single crystalline graphene grown on ru (0001) surface. *Adv. Mat.* **20**, 1. (doi:10.1002/adma.200700515)

Park, C.-H., Yang, L., Son, Y.-W., Cohen, M. L. & Louie, S. G. 2008*a* Anisotropic behaviors of massless Dirac fermions in graphene under periodic potential. *Nat. Phys.* **4**, 213. (doi:10.1038/nphys890)

Park, C.-H., Yang, L., Son, Y.-W., Cohen, M. L. & Louie, S. G. 2008*b* New generation of massless Dirac fermions in graphene under external periodic potentials. *Phys. Rev. Lett.* **101**, 126804. (doi:10.1103/PhysRevLett.101.126804)

Park, C.-H., Son, Y.-W., Yang, L., Cohen, M. L. & Louie, S. G. 2009 Landau levels and quantum Hall effect in graphene superlattices. *Phys. Rev. Lett.* **103**, 046808. (doi:10.1103/PhysRevLett.103.046808)

Pedersen, T. G., Flindt, C., Pedersen, J., Mortensen, N. A., Jauho, A.-P. & Pedersen, K. 2008 Graphene antidot lattices: designed defects and spin qubits. *Phys. Rev. Lett.* **100**, 136804. (doi:10.1103/PhysRevLett.100.136804)

Rosales, L., Pacheco, M., Barticevic, Z., León, A., Latgé, A. & Orellana, P. A. 2009 Transport properties of antidot superlattices of graphene nanoribbons. *Phys. Rev. B* **80**, 073402. (doi:10.1103/PhysRevB.80.073402)

Shytov, A. V., Abanin, D. A. & Levitov, L. S. 2009 Long-range interaction between adatoms in graphene. *Phys. Rev. Lett.* **103**, 016806. (doi:10.1103/PhysRevLett.103.016806)

Snyman, I. 2009 Gapped state of a carbon monolayer in periodic magnetic and electric fields. *Phys. Rev. B* **80**, 054303. (doi:10.1103/PhysRevB.80.054303)

Tiwari, R. P. & Stroud, D. 2009 Tunable band gap in graphene with a noncentrosymmetric superlattice potential. *Phys. Rev. B* **79**, 205435. (doi:10.1103/PhysRevB.79.205435)

Usachov, D., Dobrotvorskii, A. M., Varykhalov, A., Rader, O., Gudat, W., Shikin, A. M. & Adamchuk, V. K. 2008 Experimental and theoretical study of the morphology of commensurate and incommensurate graphene layers on Ni single-crystal surfaces. *Phys. Rev. B* **78**, 085403. (doi:10.1103/PhysRevB.78.085403)

Vázquez de Parga, A. L., Calleja, F., Borca, B., Passeggi, M. C., Hinarejos, J. J., Guinea, F. & Miranda, R. 2008 Periodically rippled graphene: growth and spatially resolved electronic structure. *Phys. Rev. Lett.* **100**, 056807. (doi:10.1103/PhysRevLett.100.056807)

Vozmediano, M. A. H., Katsnelson, M. I. & Guinea, F. 2010 Gauge fields in graphene. (http://arxiv.org/abs/1003.5179).

Wehling, T. O., Grigorenko, I., Lichtenstein, A. I. & Balatsky, A. V. 2008 Phonon-mediated tunneling into graphene. *Phys. Rev. Lett.* **101**, 216803. (doi:10.1103/PhysRevLett.101.216803)

Zhang, Y., Brar, V. W., Wang, F., Girit, C., Yayon, Y., Panlasigui, M., Zettl, A. & Crommie, M. F. 2008 Giant phonon-induced conductance in scanning tunneling spectroscopy of gate-tunable graphene. *Nat. Phys.* **4**, 627. (doi:10.1038/nphys1022)

Zhou, S. Y., Gweon, G.-H., Fedorov, A. V., First, P. N., de Heer, W. A., Lee, D.-H., Guinea, F., Neto, A. & Lanzara, A. 2007 Substrate-induced bandgap opening in epitaxial graphene. *Nat. Mater.* **6**, 770. (doi:10.1038/nmat2003)